A portable optical sensor for sea quality monitoring

F. Attivissimo, C. Guarnieri Calò Carducci, A.M.L. Lanzolla, A. Massaro, M.R. Vadrucci, "A Portable Optical Sensor for Sea Quality Monitoring", IEEE Sensors Journal ,vol: 15, no. 1, p.p. 146-153, January 2015, doi: 10.1109/JSEN.2014.2340437

A Portable Optical Sensor for Sea Quality Monitoring

Filippo Attivissimo, *Member, IEEE*, Carlo Guarnieri Calò Carducci, Anna Maria Lucia Lanzolla, *Member, IEEE*, Alessandro Massaro, *Member, IEEE*, Maria Rosaria Vadrucci

***Abstract* – In this paper we propose the modeling, the design and the development of a high sensitivity cheap optical sensor for chlorophyll *a* and water transparency based on chlorophyll fluorescence and turbidity due to scattering for in situ monitoring of trophic status of seawater. The sensor is designed in order to detect very low chlorophyll concentration and low level turbidity by means of a numeric lock-in amplifier technique, with a common resonant input stage. The sensor is designed and implemented by considering a proper layout suitable for a good light source coupling. The presented prototype integrates on a board two LED sources emitting red and blue light to measure both chlorophyll-*a* and turbidity. The system assures a chlorophyll sensitivity of 1 mV/ 2.5 μg/l, a detectivity of 0.2 μg/l, with a 40 dB minimum attenuation of all the other light sources. It is attractive with respect to commercial systems because it guarantees considerable reliability with low manufacturing costs.**

***Index Terms* — Optical sensing, lock in, fluorescence, sea water monitoring, chlorophyll.**

I. Introduction

For thousands of years the sea has been an important resource for the livelihood and well-being of European populations, but the possibility of exploiting this resource is increasingly threatened by degradation, mainly due to the pressure of human activities, as attested in international directives [1], [2]. In this context growing attention has been paid to monitor air and water pollution for reducing health risk and preserving the ecosystem [3]-[5]

In recent years, the increasing of both manufacturing industries and coastal tourism has exposed the Mediterranean Sea to great environmental pressures. On the other hand, the discharge of industrial and municipal wastewater can be considered a constant polluting source and a potential cause of alteration for the Mediterranean Sea [6], [7]. Eutrophication has been considered one of the major threats to the quality of marine ecosystems including Mediterranean.

F. Attivissimo, C. Guarnieri Calò, Carducci and A. M. L. Lanzolla are with Department of Electric and Information Engineering, Polytechnic of Bari, Italy (e-mail: attivissimo@misure.poliba.it, carlo.guarnieri@libero.it,: lanzolla@misure.poliba.it corresponding author)

A. Massaro is with Center for Bio-Molecular Nanotechnologies (CBN), Italian Institute Technology (IIT), Arnesano, Lecce-Italy (e-mail: alessandro.massaro@iit.it)

M.R. Vadrucci is *Regional* Environmental Protection Agency Puglia Lecce, Italy (e-mail: m.vadrucci@arpa.puglia.it)

It can be defined as "an increase in the rate of supply of biomass and organic matter" [8], mainly due to nutrient enrichment that stimulates the primary productivity of pelagic compartment (phytoplankton), of benthic micro and macro algae and high plants.

The eutrophication reduction is a primary objective in both Water Framework Directive (WFD-2000/60/EC) [8] and in EU Marine Strategy Framework Directive (MSFD-2008/56/EC) [8]. Chlorophyll-*a* is considered as a proxy for indirect biomass measurements in pelagic ecosystems. Chlorophyll-*a* is a pigment involved in photosynthetic processes to produce carbohydrates and life-sustaining oxygen, starting from water, carbon dioxide and sun light. It is present in phytoplankton, macroalgae and other water plants. It absorbs most energy from wavelengths of violet-blue and orange-red light. The primary effects of eutrophication are excessive growth of phytoplankton, increasing concentration of chlorophyll-*a*, increasing of the amount of organic matter settling on the bottom and reduction of water transparency[10].

As a consequence, chlorophyll-a and water transparency represent important parameters for the assessment of the quality status of marine ecosystems [11] and therefore they are included in most eutrophication monitoring programs. For this reason, Chl-*a* values have the best geographical coverage at the European level [12].

In marine ecosystems, chlorophyll-*a* concentration shows an intrinsic natural variability as on temporal scale, as on spatial local scale (inshore-offshore) and on biogeographic scale. In Mediterranean sea the average values vary between 0.2-1.5 μg/l [12] except in proximity of rivers delta or estuaries, as in the case of Po river in the Northern Adriatic sea where the increase of nutrients input promotes algae replication rising the inner chlorophyll-*a* concentration up to 8 μg/l [13].

The "*in situ*" quantification of chlorophyll *a* is based on fluorimetric methods, using optical probes that measure artificially induced phytoplankton fluorescence. Optical detection could be a good solution being the elements (photosynthetic organisms and organic and inorganic particles) to be monitored of micro-scale dimensions. Concerning large scale problems, optical probes were previously studied for other types of sea water pollution such as oil spill [14]. Often the variation of trophic status is not a visible feature as in oil spill, because it is in the chemical processes supported by micro-elements contained in the water.

Hence a way to optically evaluate this micro-environmental is to measure its chlorophyll-*a* content through chlorophyll-*a* fluorescence [15], [16].

In the market are present optical sensors based on fluorescence detection able to detect *in situ* chlorophyll-*a* [17], [18] for rivers, ocean, coastal marine area and systems for aquaculture. Nevertheless many of these are devoted to measure only chlorophyll-*a*, even if the measure principle is the same for other useful indicators, such as example Phycocyanin for freshwater application and Phycoerythrin for marine ones; generally, these devices are quite expensive, are used in oceanographic applications and requires specialized technicians for custom configurations. The sensor we propose is able instead to take advantage of common fluorescence emission ranges as well as of other optical method involving the same wavelength range (e.g. turbidity measurement), adopting a single high performance common stage, avoiding design redundancies and thus cutting costs to final users. It could be attractive for research centers or environmental protection agencies with respect to commercial systems because it guarantees good results with low incidence on the experimental setup costs. This advantage is more pronounced when a network of these sensors is required for monitoring a wide sea area. Some designers have opted to use photomultiplier input stages [19] technology to overcome the intrinsically weak light emission due to combined effects of very-low Chl-*a* concentration and its low fluorescence quantum yield, whereas our approach is based on numerical techniques able to efficiently extract the required information from a noisy environment.

On the other hand new competitive devices [20] have being developed in the recent years taking advantage of new improved electronic technologies. Though the latter is able to reach a sensitivity of 0.05 µg/l and go to a depth of 1000 m, the proposed prototype is rather intended to be an extremely cheap and reliable measurement extension for a classical CTD (Conductivity Temperature Depth) probe commonly used in oceanography, able to measure chlorophyll-*a* concentration and water turbidity. It is also IEEE 21451 [21] compliant, as it is meant to be a part of a major project, whose intent is to create a smart sensor network for *in situ* and *in continuous* space-time monitoring of surface water bodies, in particular seawater. The entire system has been designed to work at low voltage level (i.e. 3.3-5 V), with a focus on the system overall power consumption which amounted to less than 800 mW during optical emission and falls below 1 mW in standby mode, far below the 8-30 V, 3 W minimum requirements in [18].

Using standard electronic technology, we propose an alternative cheap, linear and small sensor, able to detect chlorophyll-*a* concentrations varying in a wide measurement range. This allows to use this optical sensor in marine waters characterized by low chlorophyll-*a* content (such as 0.5 – 8.0 µg/l), as well as at higher concentration level (about 200 µg/l) such as in aquaculture [22] systems or in seawater, for example Baltic Sea naturally characterized by high level of chlorophyll-*a* concentration.

II. Working Principle: A brief overview

In situ chlorophyll-*a* measurement relies on its intrinsic fluorescent property. Once the measurement sample is irradiated with blue light, it re-emits a part of the absorbed energy with higher wavelengths [23], typically in orange-red band (Fig.1).

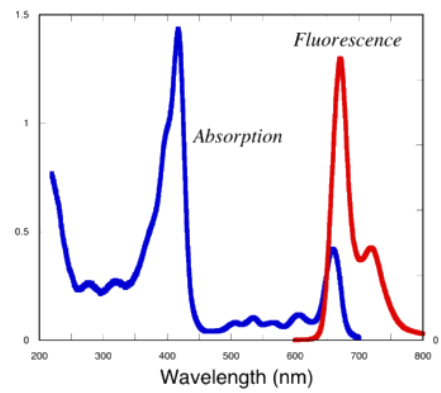

Fig.1 . Chl-a in methanol: absorption (blue line) and emission (red line) spectra in arbitrary units [24].

Thus, using a suitable light stimulus, chlorophyll-*a* molecules contained in phytoplankton cells can be induced to emit light as result of the fluorescence process, which can be subsequently collected by mean of a photodiode and used to evaluate the inner chlorophyll concentration, which can finally be used to evaluate phytoplankton concentration.

III. Measurement Background

Fluorescence is a quantum effect due to photon absorption by a molecule which induces an electron transition to an excited state. If not expended in photosynthetic processes, this excited electron could undergo a thermal dissipation, drop to a lower energy level and finally decay to ground level emitting a photon with a generally lower energy, thus with higher wavelength. The difference between absorption and emission maxima wavelengths is known as Stokes shift [23], while the ratio between emitted and absorbed photons is the fluorescence quantum yield (Φ_F):

$$\Phi_F = \frac{I_a}{I_f} \tag{1}$$

The relation between the exciting light intensity I_0 and fluorescence radiation I_f is derived by considering first the amount of light absorbed in the sample, using Lambert-Beer's equation:

$$I_a = k \cdot I_o \left(1 - e^{-\varepsilon \cdot d \cdot c}\right) \tag{2}$$

Introducing the chlorophyll fluorescence quantum yield in the above equation, leads to the final relation between absorbed light in the volume sample and the emitted fluorescence:

$$I_f = k \cdot \Phi_F \cdot I_o \left(1 - e^{-\varepsilon \cdot d \cdot c}\right) \tag{3}$$

where K is the instrumentation setup factor, ε is the molar absorption coefficient, d is the optical path and c is the

fluorescent substance concentration. Under the hypothesis of low absorbed intensity (i.e *absorbed energy < 2% of excitation energy*) and very low concentration ($\varepsilon dc < 0.01$), a new relation could also be derived linearizing equation (3), by assuming to keep constant all variables except the unknown concentration *c*.

$$I_f = K \cdot \Phi_F \cdot I_o \cdot \varepsilon \cdot d \cdot c \qquad (4)$$

Equation (4) shows a direct proportionality relation of the fluorescence intensity with Chl-*a* concentration.

Likewise in Chl-*a* fluorescence case, the nephelometric turbidity measurement also undergoes a similar linear relation. In fact the electromagnetic behavior of a wave propagating in a colloidal solution with particles dimensions comparable with excitation light wavelength is described by the Tyndall effect [23]:

$$I_s = K \cdot \frac{N \cdot V^2}{d^2 \cdot \lambda^4} \cdot I_o \qquad (5)$$

where I_s is the intensity of the scattered light, N is the number of particles for units of volume, V is the particles volume and λ is the excitation wavelength.

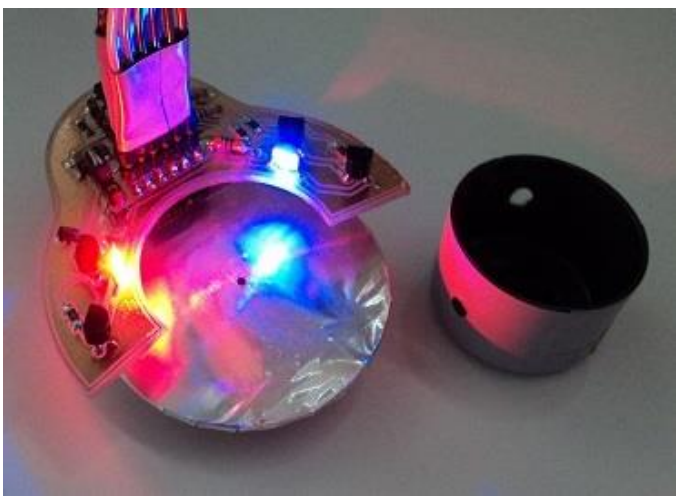

Fig.2 Photo of the optical sensor prototype.

IV. Sensor Design and Circuit

Sensor design guidelines follow the typical fluorescence measurement setup. A light source is placed to form an angle of 90 degrees with the light detector in order to avoid the stimulus light to be captured. The fluorescence signal is then collected back thanks to the isotropic emission of the sample. This setup has been also considered useful for turbidity measurement based on scattered light by suspended particles, thus using the same detector circuit with a different light stimulus. The proposed prototype is illustrated in Fig.2 representing the optical c-shaped transmitter, docked to the detection module. The optical transmitter is composed by a digitally controlled current generator, driving alternatively two LED sources (blue for Chl-*a* fluorescence excitation and red for turbidity) with a clean and stable square wave at the lock-in reference frequency.

These LEDs couple the light in the sea water sample under test. The signal coming from the light source excites the sample and the emitted or scattered amplitude modulated (AM) light is collected back on a photo-detector working in the fluorescence band range.

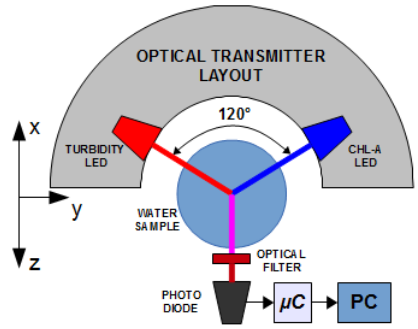

Fig.3 Scheme of measurement setup.

Because of the resonant trans impedance amplifier (TIA) input stage, only the signal generated by synchronous emission will be amplified with a gain G = 10^9, providing 40 dB of attenuation of the DC component, e.g. the sunlight.

A digital circuit will process the output signal by means of an ARM *Cortex-M3* microprocessor, the core of the *Arduino DUE* board, connected to a personal computer.

In Fig.3 the scheme of the adopted experimental setup is illustrated. The circular layout is suitable in order to facilitate the measurements; in fact the sample is inserted in the center of the circular layout for an efficient light source coupling.

The analog front end is integrated in the detection module printed circuit board (PCB), containing an anti-alias filter (see Fig.4) also useful for op-amp voltage noise integration bandwidth reduction and an analog-to-digital-converter (ADC) with SAR architecture, which communicates with the µC by means of a serial SPI connection.

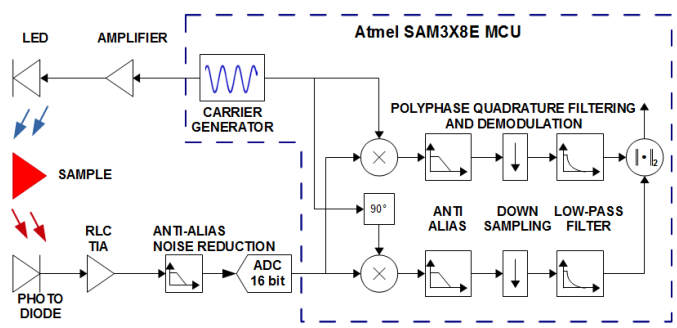

Fig.4 Simplified lock in implementation scheme.

The digital signal processing chain has been implemented to work in batch mode for debug purposes. Once the samples of the AC signal are acquired, they have to be demodulated. Hence a high performance algorithm has been implemented which makes possible anti-alias filtering, demodulation, down sampling and DC extraction of the signal, all in a single stage. Finally a variable and user-defined number of output samples are stored in the output buffer which has a default size of 1,000 samples. As last step, samples in the buffer are averaged

to provide a single measurement value and to increase the SNR by a factor of $10 \cdot \log_{10} N_s$, where N_s is the number of samples to average.

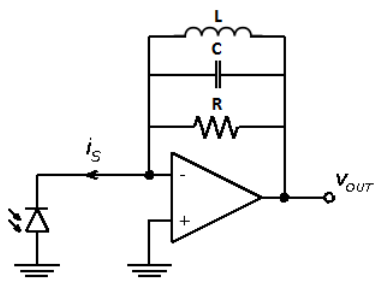

Fig.5 . RLC Trans Impedance Amplifier.

Resonant implementation of the first stage (see Fig.5) has made practicable, with respect to discrete components needed in the classical RC TIA implementation, the use of a big gain resistor while at same time keeping the synchronous AC signal bandwidth unaffected. Despite the values of resistor and capacitor involved, the inductor value for a given resonant frequency of 1 kHz and a quality factor $Q = 2\pi$ becomes now unfeasible with available discrete components, forcing its virtualization through a Miller integrator circuit (Fig.6) which well and easily emulates the behavior of an inductor between two variable voltage nodes.

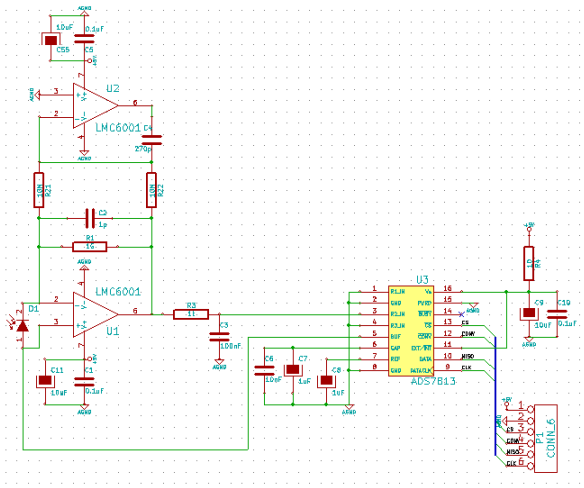

Fig.6 Detection module first prototype circuital scheme.

The inductor emulation is though incomplete and the dipole is seen as an inductor in series with the resistor used for Miller emulation, thus giving a maximum of 40 dB of attenuation of the DC component with respect to signal of interest (see Fig.7).

Using a lock-in modulation carrier of 1 kHz the signal is amplified at the output by the feedback system reported in Fig.5 able to improve the best gain of 10^9. The signal passes then through a single pole anti-alias/noise-reduction filter with a time constant $\tau = RC = 10^4$ s.

The full circuital scheme of the first prototype of optical receiver is illustrated in Fig.6, while Fig.8 shows the transmitter circuit.

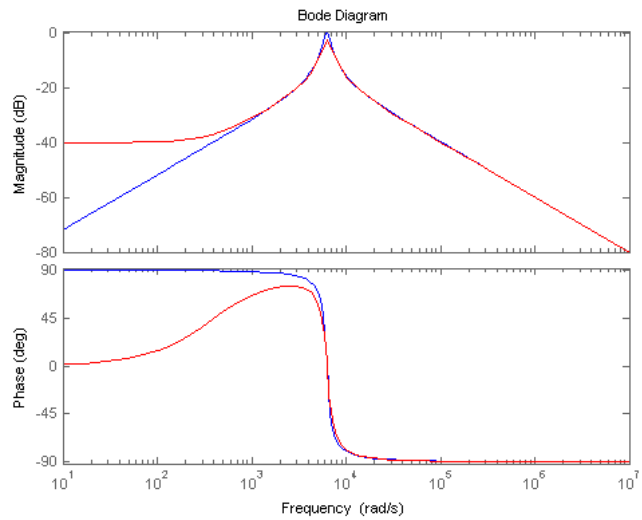

Fig.7 . Bode diagram of normalized RLC impedance, theorical (blue) and emulated through Miller integrator (red).

Through the DAC voltage, the op-amp based current generator is able to set the driving current value, in first approximation equal to the ratio of the input voltage applied to the emitter degeneration resistor. Hence a pulse width modulation (PWM) signal is used to drive alternatively the differential pair transistor bases, in order to digitally switch the LEDs at the desired frequency with a maximum percentage voltage overshoot included in range of 1-15%, inversely depending on the entity of the biasing current.

The TIA transfer function will then remove all the harmonics of the resulting square wave stimulus signal, allowing the only fundamental component to pass.

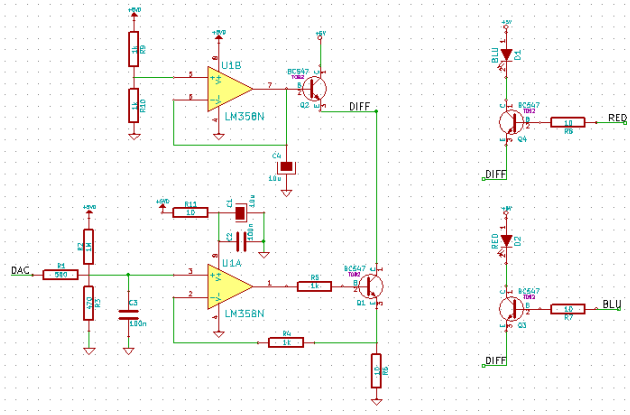

Fig.8 Transmitter module first prototype circuital scheme

V. Numerical Simulations

In order to properly design the electronic front end and to evaluate different design solutions, a careful error budget analysis of the circuit need to be performed. Hence, starting from the TIA noise model described in [25] and introducing the appropriate corrections aimed to describe and take into account the effects of the RLC stage on to the noise shape, numerical simulations have been carried out using Matlab.

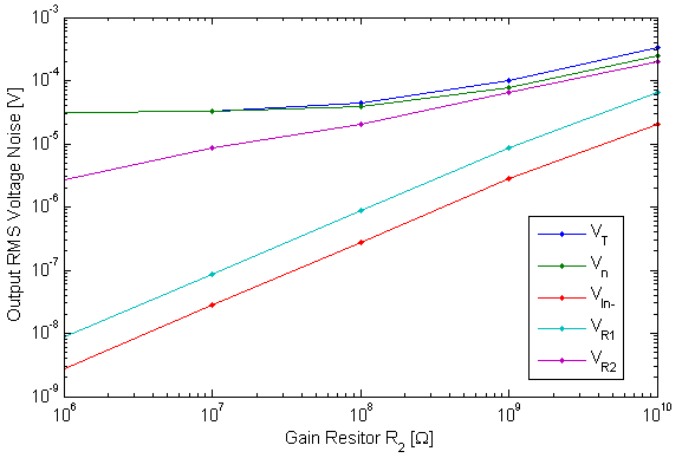

Fig.9 . Total rms TIA output noise and its components

The resulting total root means square (rms) noise, referred to TIA stage output and described in Fig.9 as function of the gain resistor, is calculated from the Euclidean norm of its uncorrelated individual rms noise components in order to properly choose a suitable ADC

$$V_T = \sqrt{\int V_n^2(f)df + \int V_{In-}^2(f)df + \int V_{R1}^2(f)df + \int V_{R2}^2(f)df} \quad (6)$$

where V_n is the op-amp voltage noise, V_{In-} is the output voltage noise due to op-amp current noise across the gain resistor R_2, V_{R1} and V_{R2} are thermal noises on R_1 photo-diode shunt resistor and R_2 gain resistor respectively.

These determined values are then used to estimate the achievable stage resolution as function of its gain. In this regard, two different resolutions are shown in Fig.10: effective resolution (ER) is calculated from the noise rms values, while the noise free code resolution (NFCR) is derived from the equivalent peak-to-peak noise, by means of the following relationships:

$$V_{PP} = 6.6 \cdot V_{rms} \quad (7)$$

$$ER = \log_2\left(\frac{FS}{V_{rms}}\right) \quad (8)$$

$$NFCR = \log_2\left(\frac{FS}{V_{PP}}\right) = \log_2\left(\frac{FS}{6.6 \cdot V_{rms}}\right) = \log_2\left(\frac{FS}{V_{rms}}\right) - \log_2 6.6 = ER - 2.7 \quad (9)$$

where FS is the sensor Full Scale and V_{rms} is the total output referred rms.

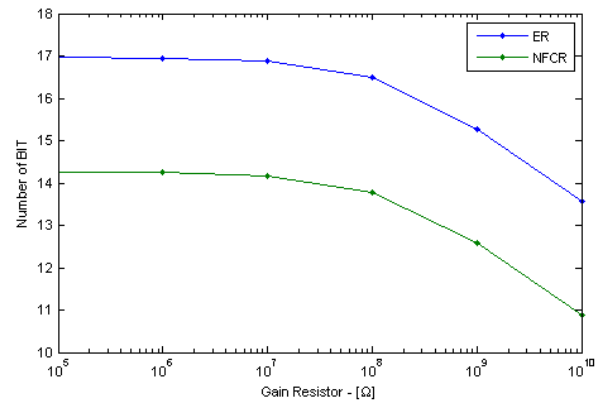

Fig.10 . Calculated number of bits

Final calculated performances of the designed input stage are reported in Table I.

Table I. Calculated RMS (NFCR) front-end performances

PARAMETER	VALUE
Total Output Noise (V_{out})[μV]	101
Max number of BITs	15,3 (12,6)
Min detectable Current [pA]	0,18 (1)

VI. Validation and Discussion

To characterize the proposed sensor it is necessary to perform experimental tests using different reference *in vivo* sea water samples with a known value of Chl-*a* concentration. The procedure required to extract the Chl-*a* concentration present in an *in vivo* sea water samples is long and complex and it has to be performed preferably in a biology laboratory. First, water samples need to be filtered through a membrane with 0.45 μm pore size to concentrate phytoplankton cells, then the filter is put in 90% acetone for 24 h at 4°C in the dark to extract chlorophyll-*a*. Samples were then centrifugate and supernatant is separate. The obtained Chl-*a* extract is then measured with a spectrophotometric or spectrofluorimetric method [26]).

Because of the complexity of the technique for extracting the Chl-*a* concentration, a Chl-*a* standard dissolved in 90% acetone with a known certified concentration of 4 mg/l (chlorophyll-*a* from *Anacystis nidulans* by SIGMA-ALDRICH) has been used to calibrate the developed sensor instead of *in vivo* sea water samples. Standard Chl-*a* concentration value was confirmed by spectrophotometic measures (spectrophotometer mod Heλios α Thermospectronic) according to the method defined by the Italian Institute of water research APAT–IRSA CNR 9020 [27].

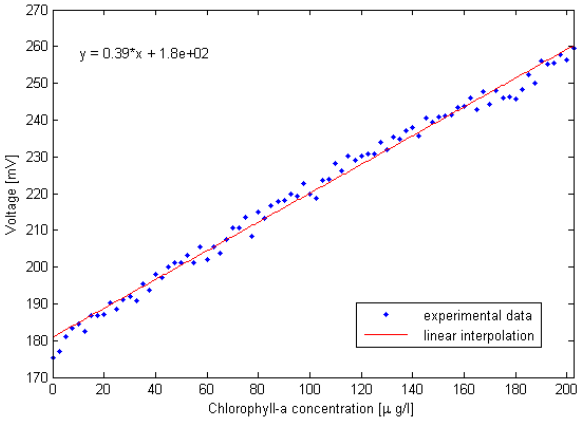

Fig.11 . Sensor calibration test performed for a LED driving current of 100 mA: blue points are experimental data, red line is the linear interpolation

In particular, the reference samples have been performed diluting in the measurement box (see Fig.2) known quantities of the certified Chl-*a* extract in known volumes of sea water (filtered through a GF/F glass filter) by using a micropipette able to dispense liquid with a precision of 1 µl. About 80 different Chl-*a* concentrations with a step of 2.5 µg/l have been prepared, so that to obtain a wide measurement range.

Fig.11 shows the calibration test results which prove a good linearity of the sensor.

An accurate calibration procedure would be useful to remove the 180 mV offset, but a solid metal structure needs first to be developed for keeping the LED to photodiode optical path at a fixed value. In fact even a half millimeter variation would affect the offset value in addition or in subtraction of several millivolts.

To validate the proposed device an analysis of measurement uncertainty based on a statistical characterization of the acquired data has been carried out according to the several studies proposed in literature on this issue [28]-[29][31]

In particular, for each referred sample provided by the Agency for the Environmental Prevention and Protection (ARPA) several experimental values have been acquired to have a significant set of data.

After a preliminary descriptive analysis of measurements, useful to investigate the dispersion of data the authors verified that the experimental measurements exhibit an approximate Gaussian distribution. According to the Guide to Expression of Uncertainty in Measurement (GUM) [32]-[34] the type A standard uncertainty was evaluated considering the average value and the sample standard deviation of the measured Clh-*a:*

$$\langle x_{Clh} \rangle = \frac{1}{N}\sum_{i=1}^{N} x_{Clh_i}$$
$$\langle \sigma \rangle = \sqrt{\frac{\sum_{i=1}^{N}(x_{Clh_i} - \langle x_{Clh} \rangle)}{N(N-1)}} \qquad (10)$$

For a Chl-*a* concentration value ranging from 0 to 200 µg/l, the standard deviation was 650 ng/l. This value is strictly correlated to lock-in amplification efficiency, to the sampling frequency, and to the adopted polyphase down sampling factor, in fact preliminary tests have shown a significant attenuation of the standard deviation when the sampling frequency increases. The $\langle \sigma \rangle$ estimation is also affected by decomposability of Chl-a molecule so a suitable protocol able to accounts this effect is advisable to reduce these fluctuations.

In order to evaluate the behavior of proposed device as function of turbidity, experimental tests have been performed adding in a sample of seawater a substance with particle size of about 1 µm to simulate the turbidity effect [34].

For this purpose, a progression of known milled flour quantities (varying in the range 0-0.25 mg with step of 0.05 mg) has been solved in a 12 ml of seawater, repeating the tests three times. For each flour increment the output voltage has been measured as shown in Fig.12. Results show a good linearity of the measured values, excepting for the last sample because of amplifier saturation.

VII. Perspectives: Sensor Housing for *in situ* Monitoring

The proposed sensor can be integrated in an embedded system for *in situ* measurements of different quantities useful to evaluate effectively the state of seawater quality. The 3D layout of the designed case is illustrated in Fig.13.

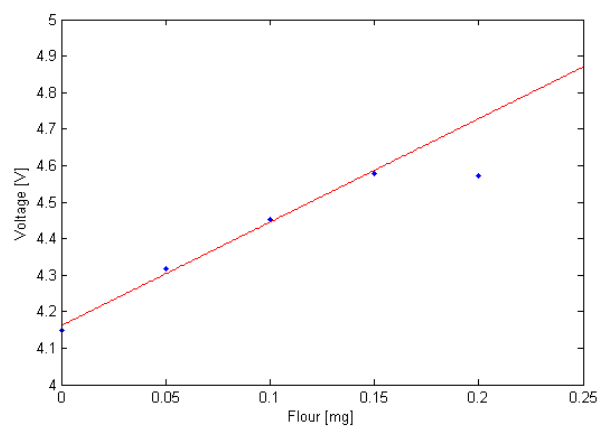

Fig.12 . Relationship between applied flours and voltage output of the developed sensor: blue dots are the measured values, red line is the linear interpolation

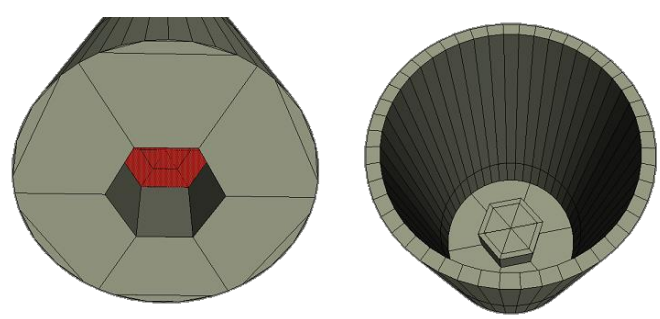

Fig.13 . Draft of the sensor housing layout without details

The hexagonal cavity has been thought to let 3 different optical measurements: chlorophyll-*a*, turbidity and a third optical slot for future functionality, such as for instance phycocyanin fluorescence, as a quality indicator in fresh waters reservoirs. LEDs are meant to be placed on alternate faces, while a slit in top of the cavity will let the light signal to reach the photodiode.

This case will also integrate a pressure sensor indicating the actual depth, allowing automatic data acquisition at fixed depth increment.

The power supply could be even 3.3 V or 5 V, making it possible to equip the sensor with a battery pack with no more need to transmit the power from the surface. Data can thus be stored inside the sensor and transmitted back through a Near Field Communication device once the user gets the sensor outside the water, or an optical transmission system may be implemented, depending on its scope.

VIII. Conclusion

We have designed and implemented a cheap, linear and high sensitivity sensor able to measure chlorophyll-*a* concentration in a very wide measurement range. This allows using the same sensor for assessing of water quality in marine areas with very different trophic conditions.

Further investigation will be addressed in rising LEDs direct current to 1 A in order to increase the sensitivity and adapting the sensor to work in real-time instead of in batch mode: this should free a lot of μC resources that can be used to increase sampling frequency and thus lock-in efficiency.

Acknowledgment

The authors would like to thank Dr. Nicola Ungaro, Environmental Manager and Marine Biologist of the Regional Agency for the Environmental Prevention and Protection, for the valuable cooperation of the Department he's in charge of to this work.

References

[1] Marine Strategy framework Directive (MSFD 2008/56/EC).

[2] European Environment Agency "Marine Messages", 2014.

[3] A. Lay-Ekuakille, A. Trotta, "Predicting VOC concentration measurements: cognitive approach for sensor networks", IEEE Sensors Journal, vol 11, pp 3030–3923, 2011.

[4] G. Andria, G. Cavone, A. M. L. Lanzolla, "Modelling Study for Assessment and Forecasting Variation in Urban Air Pollution", Measurement, vol.41, pp. 222-229, 2008.

[5] G. Andria, G. Cavone,V. Di Lecce, A. M. L. Lanzolla, "Model Characterization of Measurement Environmental Pollutants via data Correlation of Sensor Output", IEEE Trans, on Instrumentation and Measurement, vol. 54, pp. 1061-1066, 2005.

[6] F.Adamo, C. De Capua, P. Filianoti, A. M. L. Lanzolla, R. Morello, "A Coastal Erosion Model to Predict Shoreline Changes", Measurement, vol. 47, pp. 734-740, 2014.

[7] F. Adamo, G. Andria, G. Cavone, C. De Capua, A. M. L. Lanzolla, R. Morello, M. Spadavecchia, "Estimation of ship emissions in the port of Taranto", Measurement, vol. 47, pp. 982–988, 2014.

[8] Directive 2000/60/EC of the European Parliament and of the Council establishing a framework for the Community action in the field of water policy, 23 October 2000.

[9] Directive 2008/56/Ec of the European Parliament and of the Council of 17 June 2008, http://eur-lex.europa.eu/LexUriServ/LexUriServ.do?uri=OJ:L:2008:164:0019:0040:EN:PDF

[10] S.W Nixon, "Coastal marine eutrophication: a definition, social causes, and future concerns" Ophelia, vol.41, pp.199–219, 1995.

[11] M.R.Vadrucci, E.Stanca, C.Mazziotti, S.F.Umani, A.Georgia, S.Moncheva, A.Romano, R.Bucci, N.Ungaro, A.Basset, "Ability of phytoplankton trait sensitivity to highlight anthropogenic pressures in Mediterranean lagoons: A size spectra sensitivity index (ISS-phyto)", Journal of Ecological Indicators, vol 34, pp. 113–125, 2013.

[12] Italian Ministerial Decree 2010/11/8 n.260/2010.

[13] F. Giovanardi, R A. Vollenweider "Trophic conditions of marine coastal waters: experience in applying the Trophic Index TRIX to two areas of the Adriatic and Tyrrhenian seas", Journal of Limnology, vol.63, no.2, 2004.

[14] A. Massaro, A. L. Ekuakille, D. Caratelli, I. Palamara, F. C. Morabito "Optical Performance Evaluation of Oil Spill Detection Methods: Thickness and Extent by Fiber Optical Sensor," IEEE Trans, on Instrumentation and Measurement, vol. 61, pp. 3332-3339, 2012.

[15] M. Babin, A. Morel, B. Gentili, "Remote Sensing of Sea Surface Sun-induced Chlorophyll Fluorescence Consequences of Natural Variations in the Optical Characteristics of Phytoplankton and the Quantum Yield of Chlorophyll a Fluorescence", Int. J. Remote Sensing, vol. 17, pp. 2417-2448, 1996.

[16] A. A. Fernandez-Jaramillo, C. Duarte-Galvan, L. M. Contreras-Medina, I. Torres-Pacheco, R. de J. Romero-Troncoso, R. G. Guevara-Gonzalez, and J. R. Millan-Almaraz, "Instrumentation in Developing Chlorophyll Fluorescence Biosensing: A Review," Sensors, vol. 12, pp. 11853-11869, 2012.

[17] http://www.ysi.com/media/pdfs/E39-6025-Chlorophyll-Sensor.pdf.

[18] http://www.turnerdesigns.com/t2/doc/brochures/S-0143.pdf.

[19] http://www.turnerdesigns.com/t2/doc/appnotes/998-5101.pdf.

[20] Yi-min Yang, Kai-kai Lou, Le-chuan Zhou and Shu-ming Ye, "Design of A High-Sensitivity, Low-Power Instrument for Chlorophyll A Measurements", 3rd International Conference on Biomedical Engineering and Informatics, pp. 1450-1454, 2010.

[21] IEEE Standard for a Smart Transducer Interface for Sensors and Actuators—Transducer to Microprocessor Communication Protocols and Transducer Electronic Data Sheet (TEDS) Formats, IEEE Standard 1451.2–1997, IEEE, The Institute of Electrical and Electronics Engineers, Inc., NY, 1997

[22] K. Kunlasak, C. Chitmanat, N. Whangchai, J. Promya, L. Lebel, "Relationship of Dissolved Oxygen with Chlorophyll-a and Phytoplancton Composition in Tilapia Ponds", *International Journal of Geosciences*, 2013, 4, 46-53.

[23] Joseph R. Lakowicz "Principles of Fluorescence Spectroscopy" Springer, 2006.

[24] http://biologywiki.apps01.yorku.ca/index.php?title=Main_Page/BIOL_4160/Fluorescence_and_Reaction_Centers&oldid=858

[25] W. Kester, “Practical Design Techniques for Sensor Signal Conditioning”, Analog Devices Technical Reference Books, vol. 5, pp. 1-40, 1999.

[26] S.W. Jeffrey, R.F.C. Mantoura S.W Wright “Phytoplankton pigments in oceanography: guidelines to modern methods”, Monographs on Oceanographic Methodology, UNESCO 1997.

[27] APAT-IRSA-CNR “Determinazione della clorofilla: Metodo Spettrofotometrico”, Manuali e Linee Guida 29/2003, pp1137-1142.

[28] L. Angrisani, M. D’Apuzzo, R.Schiano,Lo Moriello, “New proposal for uncertainty estimation in indirect measurements”, IEEE Trans. on Instr. and Meas., vol.55, No.4, Agosto 2006

[29] A. Ferrero, S. Salicone,”Measurement uncertainty”,IEEE Instrumentation and Measurement Magazine ,Vol. 9, no 3, June 2006, Pages 44-51.

[30] F Attivissimo, A Cataldo, N Giaquinto, M Savino “Assessment of the uncertainty associated with systematic errors in digital instruments: an experimental study on offset error” Meas. Sci. Technol. 23 (2012)

[31] L.Angrisani, M.D’Apuzzo, R.Schiano Lo Moriello, “The unscented transform: a powerful tool for measurement uncertainty evaluation”, IEEE Trans. on Instr. and Meas., vol.55, No.3, 2006, pp.737-743

[32] International Organization for Standardization, “Guide to the Expression of Uncertainty in Measurement (GUM)”, first ed., ISO, 1993, (withdrawn).

[33] International Organization for Standardization, 2008, “Uncertainty of Measurement – Part 3: Guide to the Expression of Uncertainty in Measurement (GUM), ISO, 2008.

[34] American Public Health Association, American Water Works Association, Water Environment Federation, "Standard Methods for the Examination of Water and Wastewater" 1999

[35] International Organization for Standardization, ISO/IEC Guide 99:2007, “International Vocabulary of Metrology-Basic and General Concepts and Associated Terms (VIM), ISO, 2007.